

Investigation of Void Nucleation and Propagation in the Joule Heating Effect During Electromigration in Flip-Chip Solder Joints

Y.W. CHANG,¹ S.H. CHIU,¹ and CHIH CHEN^{1,2}

1.—Department of Materials Science and Engineering, National Chiao Tung University, Hsin-chu 30010, Taiwan, Republic of China. 2.—e-mail: chih@mail.nctu.edu.tw

This study analyzes the effect of void propagation on the temperature increase of solder joints by using x-ray microscopy, Kelvin probes, and infrared microscopy. It was found that the temperature rise due to void formation was less than 1.3°C when the voids depleted about 75% of the contact opening, even though bump resistance had increased to 10.40 times its initial value. However, the temperature rose abruptly with an increase of up to 8.0°C when the voids depleted 96.2% of the contact opening. A hot spot was observed immediately before the occurrence of open failure in the solder bump. The local increase in temperature was about 30.2°C at the spot. This spot may be the remaining contact area immediately before the occurrence of open failure.

Key words: Electromigration, flip-chip solder joints

INTRODUCTION

With rapid increases in packaging density and higher performance of portable devices, flip-chips have been adopted due to their excellent electrical performance and superior heat-dissipation ability.¹ Electromigration (EM) has become an important reliability issue for flip-chip solder joints.^{2,3} As the demand for high-performance electronic applications increases, the current density in flip-chip solder bumps continues to increase as well.⁴ Under the application of high currents, the Joule heating effect in solder bumps has also become significant in accelerated EM tests. Due to the current-crowding effect during EM, voids nucleate in the solder bump near the entrance of the electron flow. With increased stressing time, voids grow and propagate along the interface between under bump metallization (UBM) and solders. The evolution of Joule heating at various stages of void formation is of wide interest. Since local Joule heating increases the temperature of solder bumps, faster diffusion at high temperatures is to be expected. Thus, serious Joule heating accelerates the process of void formation, and when voids deplete the entire contact

opening, open failure occurs. Liang et al.⁵ performed finite-element simulation to explore the effect of void propagation on the Joule heating of solder bumps. They reported that the temperature did not obviously increase before voids depleted 80% of the contact opening. Even when the voids had depleted 96% of the contact opening, there was only about a 1°C increase. Tsai et al.⁶ measured the temperature on a Si-die surface during EM, and they found that the temperature increased by about 2°C during the middle stage of EM. There was an abrupt increase in temperature to 75°C during the final stage of EM. However, void size was not correlated with the temperature increase.

In this study, infrared (IR) microscopy was employed to measure the temperature in an Al pad directly above the solder bump during various stages of EM. X-ray microscopy was used to map the void location and size. Kelvin bump probes were utilized to detect the bump resistance during current stressing. Thus, temperature increases in the solder bump could be correlated with void size and bump resistance during different stages of void propagation.

EXPERIMENTAL PROCEDURES

To facilitate x-ray observation of void formation, flip-chip solder joints with a low bump height were used in this study.⁷ Figure 1 shows a cross-sectional

(Received May 2, 2010; accepted August 9, 2010; published online September 10, 2010)

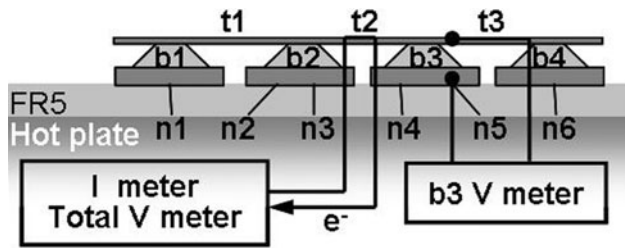


Fig. 1. Cross-sectional schematic of the layout design. The Al trace connected all four solder bumps together. The resistance of bump b3 can be measured using the experimental setup.

schematic of a Sn-Pb solder bump with $5\ \mu\text{m}$ Cu/ $3\ \mu\text{m}$ Ni UBM. The bump height is about $25\ \mu\text{m}$. The passivation and UBM opening are $85\ \mu\text{m}$ and $120\ \mu\text{m}$, respectively. On the substrate side, $5\ \mu\text{m}$ electroless Ni was adopted as a metallization layer.

Kelvin bump probes were employed to monitor the bump resistance during EM.⁸ Figure 1 shows a cross-sectional schematic of the structure. The test structure consisted of four bumps, which were connected by an Al trace. The four bumps were labeled bump 1 through bump 4. The Al trace was $1.5\ \mu\text{m}$ thick and $100\ \mu\text{m}$ wide. The pitch of the solder joints was $1\ \text{mm}$. Six Cu lines on the FR4 substrate were connected to the four bumps, labeled nodes 1 through 6, as shown in the figure. The Cu lines were $30\ \mu\text{m}$ thick and $100\ \mu\text{m}$ wide. With these six Cu lines, various experimental setups can be used to measure the bump resistance for bump 2 or bump 3, or the resistance for the middle segment of the Al trace. In this study, current was applied through nodes 3 and 4, i.e., electrons flowed from the chip side to the substrate side for bump 3 and in the opposite direction for bump 2, as illustrated in Fig. 1. In general, a void is formed in the chip side of bump 3 due to the serious current-crowding effect. In this study, the voltage change in bump 3 was monitored through nodes 5 and 6. Therefore, the change in bump resistance during EM for the bump with electron flow downward can be monitored. With the aid of Kelvin probes, one can terminate the current stressing at the desired stages accurately. The power supply used in this measurement was a Keithley 2400, which has a $0.1\ \mu\text{V}$ resolution in voltage measurement. The error in measuring resistance in this study was estimated to be $1\ \mu\Omega$ to $10\ \mu\Omega$.

EM was conducted with a current of $0.8\ \text{A}$ at 150°C on a hot plate. When the bump resistance increased to a desired value, current stressing was terminated. Then an x-ray microscope (Dage XL-6500) was utilized to map the distribution of voids in bump 3. The x-ray detector had a spatial resolution of $2\ \mu\text{m}$. Temperature increases due to void formation were measured by using an IR microscope (Infra-scope II, Quantum Focus Instrument), which had a $2.8\ \mu\text{m}$ spatial resolution. Both inspection techniques were nondestructive and were performed from the chip

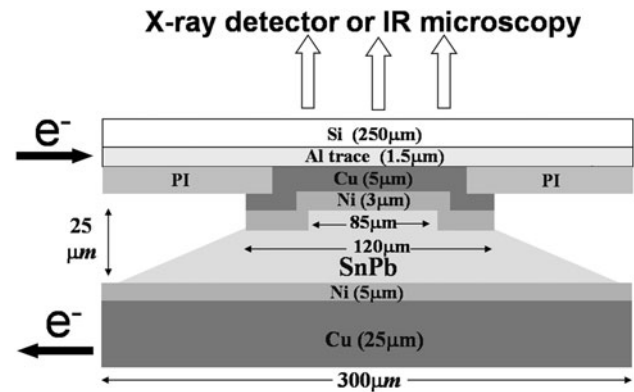


Fig. 2. Cross-sectional schematic diagram of the solder joints used in this study. X-ray microscopy was employed to measure the area of the voids, and IR microscopy was used to monitor the temperature changes due to void formation.

surface, as illustrated in Fig. 2. For the temperature measurement by the IR microscope, the same current was applied to the solder bump placed on a hot stage at 100°C . This allowed temperature increases due to void formation to be obtained. An EM test was applied again to help voids grow and propagate to a desired stage. The distribution of voids and increases in temperature were measured again using the x-ray and IR microscopes. The procedures were repeated until open failure occurred in the solder bump. Therefore, it was possible to obtain the increase in temperature as a function of void size, bump resistance, and stressing time.

RESULTS AND DISCUSSION

The x-ray microscope was able to map the voids during various stages of EM. Figure 3a–d shows x-ray images for a solder bump stressed by $0.8\ \text{A}$ at 150°C for $0\ \text{h}$, $50.0\ \text{h}$, $941.4\ \text{h}$, and $1087.9\ \text{h}$, respectively. The corresponding bump resistances were 1.0 , 1.2 , 10.4 , and 23.7 times their initial values. Electrons entered the contact opening from the Al trace on the left-hand side. So, voids started to form at that location. The contrast at the voids appears brighter than the contrast without voids. The inner dotted white circle represents the passivation opening, whereas the outer white circle indicates the UBM opening. The outer dark circle denotes the Cu pad on the substrate side. There, before current stressing, no obvious voids were observed, as shown in Fig. 3a. The contrast within the inner circle is dark and uniform, indicating that no voids were present at this stage. Voids grew and propagated as the stressing time increased. After current stressing for $50.0\ \text{h}$, the bump resistance increased to 1.2 times its initial value. The electrons entered bump 3 from the left-hand side of the passivation opening. A clear white patch can be observed near the entrance point of the electron flow, as depicted in Fig. 3b. This patch represents the void formation in this region, because the

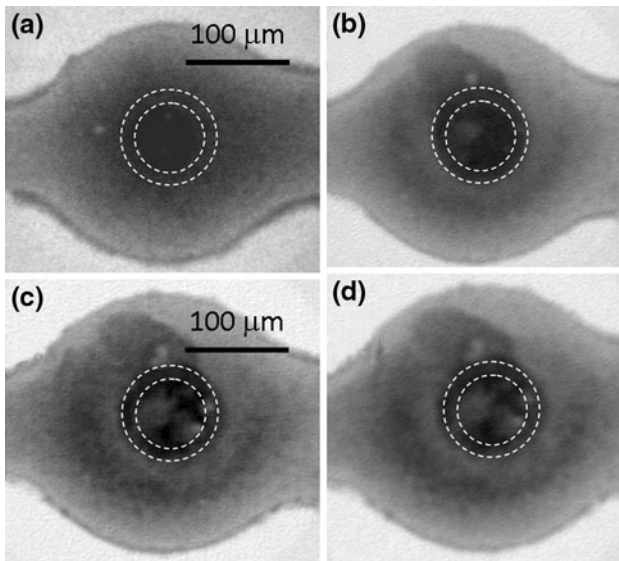


Fig. 3. Plan-view x-ray images of the same joint after stressing for (a) 0 h, (b) 50.0 h, (c) 941.4 h, and (d) 1087.9 h. The UBM and passivation openings are labeled by dotted white circles.

contrast of the x-ray image becomes brighter with void formation. As the stressing time increased, the voids continued to propagate toward the rest of the UBM opening, as illustrated in Fig. 3c and d. The bump resistance increased as voids propagated to deplete the UBM opening. Software was employed to measure the area of the voids. The corresponding

depletion percentages of the UBM opening area were 0%, 41.3%, 75.2%, and 94.1% for the four stages.

Increases in temperature were measured at the four stages by using an IR microscope. The temperature in the Al pad directly above the stressed solder bump can be detected by the IR microscope, since the 250 μm Si is transparent to IR. In addition, the Al pad was connected to the UBM and solder bump, thus the measured temperature was very close to that of the bump. The average temperature was obtained by averaging the data points in a square of 40 μm × 40 μm, as labeled in Fig. 4a. Figure 4a–d shows corresponding temperature maps for the four stages in Fig. 3. The electrons entered the bump from the Al trace on the left-hand side, and there was no current flowing in the Al trace on the right-hand side. Thus, the temperature in the Al trace on the left-hand side was slightly higher than that on the right-hand side. The temperature increased slowly with stressing time. Figure 4a shows a temperature map of the Al trace directly above bump 3 at the very beginning of current stressing. The average temperature at the Al pad is about 114.5°C, which indicates a Joule heating effect of 14.5°C. When the voids had depleted 41.3% of the UBM opening, the average temperature increased only to 115.2°C, as depicted in Fig. 4b. Figure 4c illustrates the temperature map of the Al trace as the voids grew to deplete 75.2% of the UBM opening. The average temperature was only 115.8°C. The temperature increased obviously when the voids

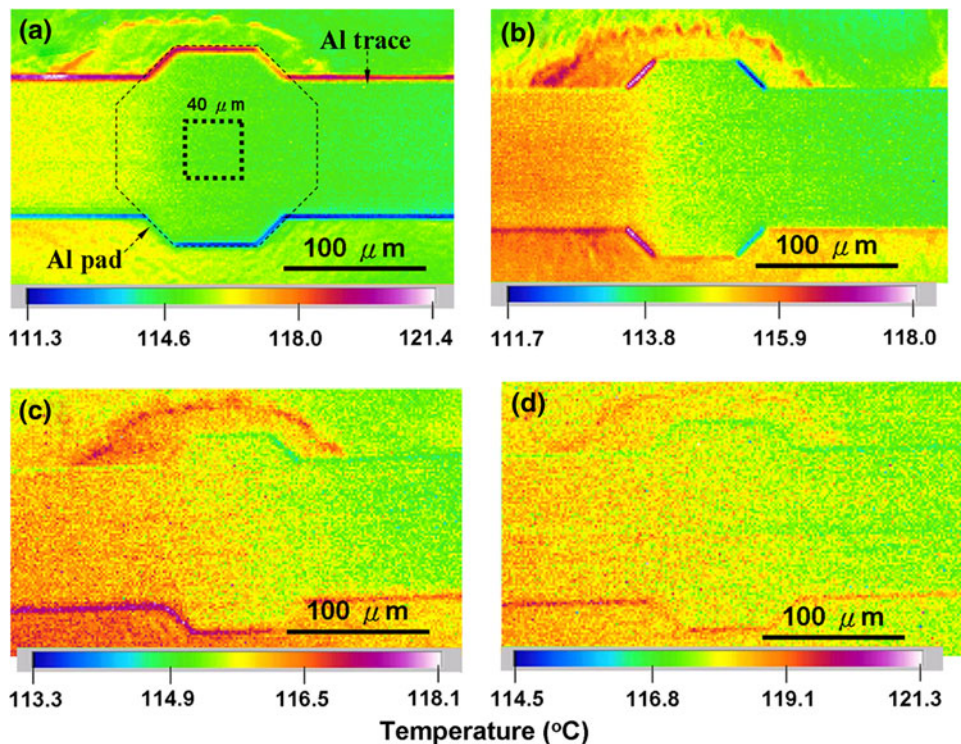


Fig. 4. IR images of the temperature distribution on the Al pad after stressing for (a) 0 h, (b) 50.0 h, (c) 941.4 h, and (d) 1087.9 h. The corresponding bump resistances are 1.0, 1.2, 10.4, and 23.7 times their initial value.

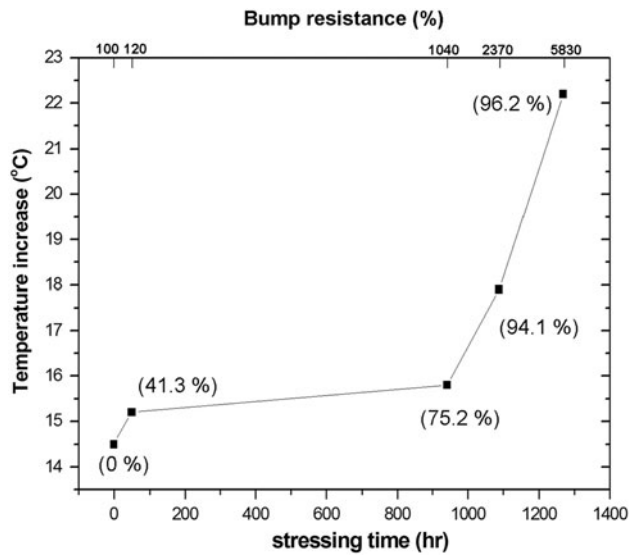


Fig. 5. Average increase in temperature at various stages. The bump resistance is labeled at the upper x-axis, and the depletion percentage of UBM opening is shown by data points.

occupied 94.1% of the UBM opening, as shown in Fig. 4d. The mean temperature was approximately 117.8°C.

Figure 5 presents the average temperature as a function of stressing time and bump resistance. The depletion percentage is also labeled on the data points in the figure. It is found that the temperature does not increase much before voids deplete 75.2% of the UBM opening. The temperature only increases 1.3°C when the voids deplete 75.2% of the passivation, that is, when the bump resistance increases to 10.4 times its original value. It is quite interesting that the temperature increase is very small even when the voids deplete 75.2% of the passivation. This is because the major heating source is the Al trace. The resistance of the Al trace is 330 mΩ, whereas the bump resistance is about 5 mΩ. In addition, the local maximum current density in the solder may not increase much even though voids deplete 75.2% of the UBM opening.⁵ Therefore, local Joule heating in the solder may not increase much before this stage.

However, the temperature increases significantly during the very late stages. When voids depleted 94.1% and 96.2% of the UBM opening, the increases in temperature were 17.8°C and 22.2°C, respectively. The abrupt temperature increase may be due to two reasons: first, the bump resistances increased to 23.7 and 58.3 times their original value. Thus, Joule heating from the solder bump is capable of contributing to the increase of temperature. Another reason lies in the local Joule heating in solders, which may also contribute significantly to the rise in temperature. At the final stage, the remaining contact area was only 3.8% of the original value. Thus, serious current crowding is expected to occur at this stage, resulting in obvious increase in temperature.

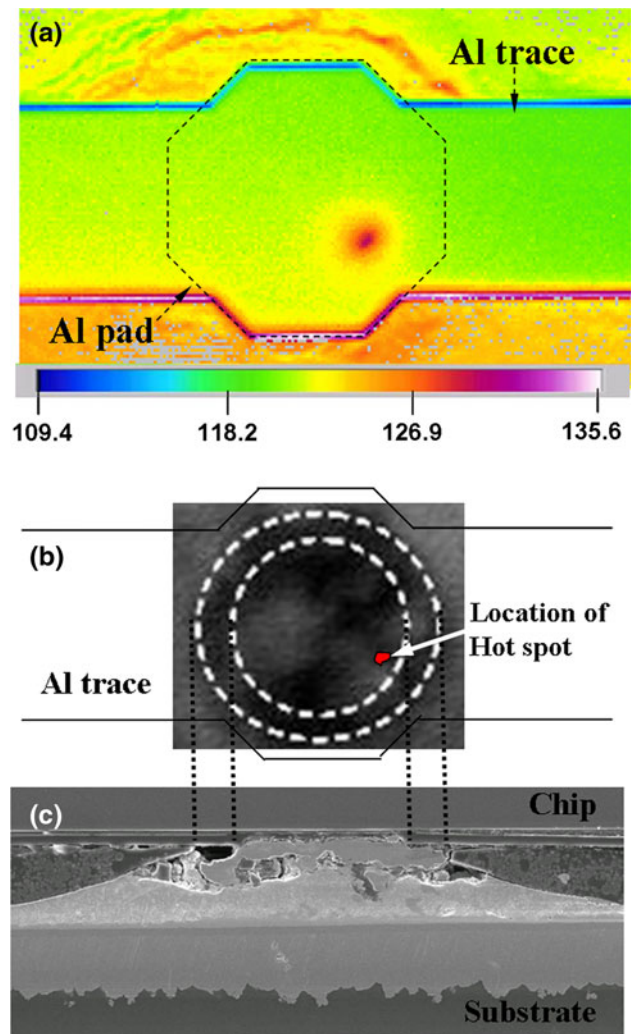


Fig. 6. (a) IR image showing the temperature distribution on the Al pad after stressing for 1267.9 h. Open failure took place immediately after the temperature measurement. (b) The x-ray image of the solder joints. The position of the hot spot is labeled on the figure. (c) Cross-sectional SEM image showing the position of voids for failed joints.

It is intriguing that a hot spot was observed on the Al pad immediately before the occurrence of open failure. Figure 6a presents the temperature map on the Al pad after current stressing for 1267.9 h. The bump resistance had increased to 58.3 times its original value before the temperature measurement by the IR microscope. Open failure took place during this measurement. The local increase in temperature was about 30.2°C at the spot. This spot should be the remaining contact area immediately before the occurrence of open failure. To further identify the location of the spot, an x-ray image and cross-sectional microstructure analysis were performed, as shown in Fig. 6b and c. The positions of the passivation opening, UBM opening, and Al trace are marked in Fig. 6b. In addition, the location of the hot spot is also labeled on the figure. The bump was polished laterally to approximately

the location of the hot spot and was examined by scanning electron microscopy (SEM). Voids depleted almost the entire UBM opening. The location of the hot spot may be the final conducting path before open failure takes place. Furthermore, the local increase in temperature may induce local melting of the solder.⁶ When a stringent stressing condition is applied, more severe local Joule heating may take place before failure. When local temperatures exceed the melting point of the solder, local melting will occur at this final stage.

It is interesting that the Joule heating effect did not increase much until the voids depleted over 75% of the UBM opening. As described above, the temperature increase is approximately 1.3°C when the voids occupied 75% of the UBM opening. To verify if these results are reasonable, a three-dimensional simulation using finite-element analysis was carried out to verify the evolution of the current density distribution due to void formation. The detailed information for the simulation model was reported in our previous publication.⁸ Figure 7a illustrates the current density distribution without void formation when the solder joint was subjected to 0.8 A current stressing. The dimension and the structure of the solder joint are almost identical to those used in this study. Current crowds into the solder joint from the upper-left corner. The maximum current density is 2.4×10^4 A/cm² inside the solder bump. As the voids grow, the current redistributes due to the void formation. Figure 7b depicts the distribution of current density when the voids deplete 74.5% of the UBM opening, which is very close to the case in Fig. 3c. Due to the void formation, the current needs to drift farther along the Al pad and then is able to enter the solder bump, resulting in the increase in bump resistance. The maximum current density in the solder bump increases to 7.5×10^4 A/cm², which is about a 312% increase compared with the value without void formation. This increase in maximum current density also induces local Joule heating. However, the Al trace serves as the major contributor to overall Joule heating. The current density was as high as 5.3×10^5 A/cm² in the Al trace. As mentioned above, the resistance of the Al trace overwhelms the bump resistance. Therefore, the increase in bump resistance and maximum current density did not contribute a significant temperature increase at this stage. As the voids further deplete the UBM opening, both the bump resistance and maximum current density increase abruptly. Figure 7c presents the current density distribution in solder joints with depletion of 91.8% of the contact opening. Only a small contact opening remained for current conduction. The maximum current density increased abruptly to 2.2×10^5 A/cm². Then, the local Joule heating effect in the solder joint will become pronounced and the temperature in the solder joints increased rapidly.

To further examine the relationship between the remaining contact area and the resistance change,

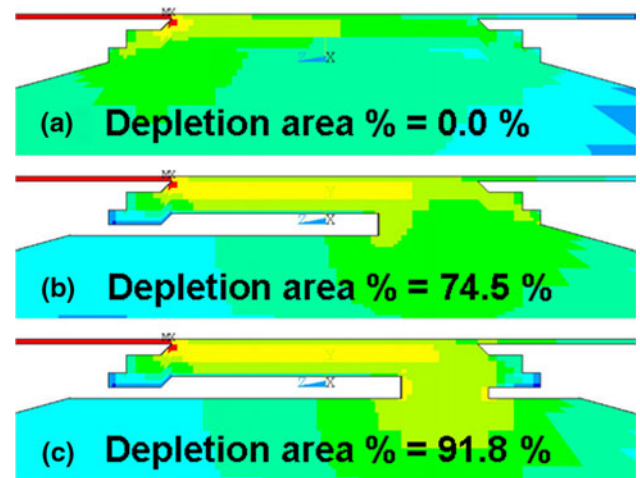


Fig. 7. Cross-sectional view showing the simulated distribution of current density in the solder joints subjected to a 0.8 A current stressing: (a) without void formation, (b) with voids depleting 74.5% of the UBM opening, and (c) with voids depleting 91.8% of the UBM opening.

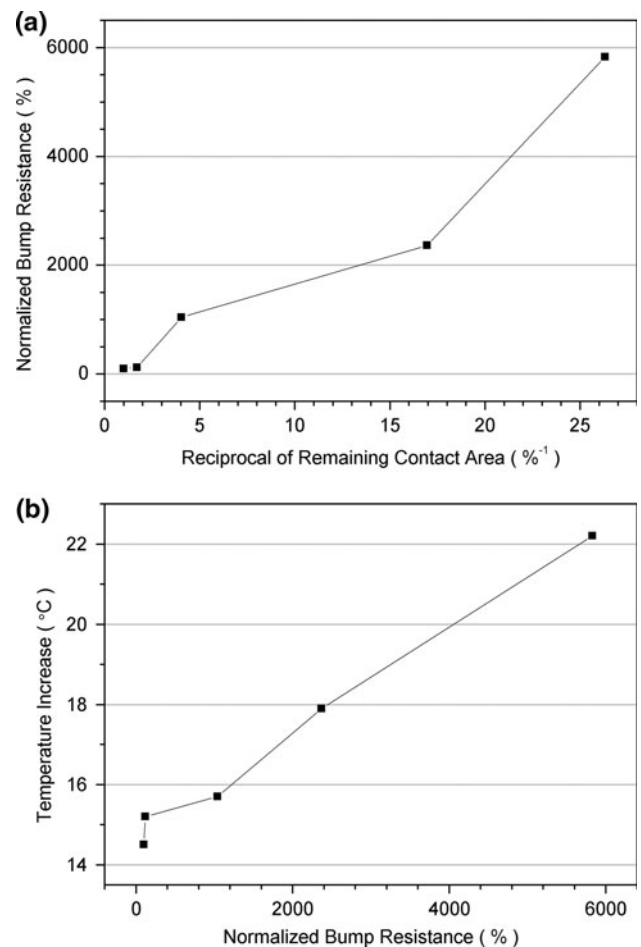


Fig. 8. (a) Plot of normalized bump resistance against the reciprocal of remaining contact area. (b) Plot of temperature increase in the solder bump against normalized bump resistance.

the normalized bump resistance was plotted against the reciprocal of the remaining contact area, as depicted in Fig. 8a. The curve shows a linear relationship, which suggests that the bump resistance is inversely proportional to the contact area; i.e., the resistance rise is mostly induced by contact area change. In addition, the temperature increase was plotted as a function of normalized bump resistance to investigate how the bump resistance affects the Joule heating effect. Figure 8b illustrates the curve; approximately linear behavior is observed. In general, the Joule heating power can be expressed as

$$P = I^2 R, \quad (1)$$

where P is the Joule heating power, I is the current, R is the total resistance of the circuit.

The curve in Fig. 8b also follows the relationship in Eq. 1. The temperature increase in the solder bump is mainly induced by the increase in bump resistance.

CONCLUSIONS

With the aid of x-ray microscopy, Kelvin probes, and IR microscopy, the effect of void propagation on temperature increase has been investigated in flip-chip solder joints. It is found that the temperature increases very slowly until voids deplete 75% of the UBM opening. However, it increases abruptly afterwards, due to a rapid increase in the local current density. The maximum current density increased

from 2.4×10^4 A/cm² to 2.2×10^5 A/cm² as the voids depleted 91.8% of the contact opening. A hot spot is observed immediately before the occurrence of open failure, which may induce local melting of the solder at the final stage of EM in flip-chip solder joints. The results indicate that the increase in bump resistance is mainly caused by the reduction in the contact area, and the temperature increase in the solder bump is mostly induced by the increase in bump resistance.

ACKNOWLEDGEMENT

The authors would like to thank the National Science Council of the Republic of China, Taiwan, for financially supporting this research under Contract No. 95-2221-E-009-088MY3.

REFERENCES

1. *International Technology Roadmap for Semiconductors, Assembly and Packaging Section* (San Jose, CA: Semiconductor Industry Association, 2007).
2. K.N. Tu, *J. Appl. Phys.* 94, 5451 (2003).
3. C. Everett, C. Yeh, W.J. Choi, and K.N. Tu, *Appl. Phys. Lett.* 80, 580 (2002).
4. C.Y. Liu, C. Chen, C.N. Liao, and K.N. Tu, *Appl. Phys. Lett.* 75, 58 (1999).
5. S.W. Liang, Y.W. Chang, T.L. Shao, C. Chen, and K.N. Tu, *Appl. Phys. Lett.* 89, 022117 (2006).
6. C.M. Tsai, Y.L. Lin, J.Y. Tsai, Y.S. Lai, and C.R. Kao, *J. Electron. Mater.* 35, 1005 (2006).
7. S.H. Chiu and C. Chen, *Appl. Phys. Lett.* 89, 262106 (2006).
8. Y.W. Chang, S.W. Liang, and C. Chen, *Appl. Phys. Lett.* 89, 032103 (2006).